

Published in final edited form as:

Eur Urol. 2011 May ; 59(5): 784–796. doi:10.1016/j.eururo.2011.02.033.

Shock Wave Technology and Application: An Update[★]

Jens J. Rassweiler^{a,*}, Thomas Knoll^b, Kai-Uwe Köhrmann^c, James A. McAteer^d, James E. Lingeman^e, Robin O. Cleveland^f, Michael R. Bailey^g, and Christian Chaussy^h

^aDepartment of Urology, Klinikum Heilbronn, SLK Kliniken Heilbronn, University of Heidelberg, Heilbronn, Germany

^bDepartment of Urology, Klinikum Sindelfingen-Böblingen, Klinikverbund Südwest, University of Tübingen, Tübingen, Germany

^cDepartment of Urology, Theresienkrankenhaus Mannheim, University of Mannheim, Mannheim, Germany

^dDepartment of Anatomy and Cell Biology, Indiana University School of Medicine, Indianapolis, Indiana, USA

^eMethodist Hospital Institute for Kidney Stone Disease, Indianapolis, Indiana, USA

^fDepartment of Mechanical Engineering, Boston University, Boston, Massachusetts, USA

^gApplied Physics Laboratory, University of Washington, Seattle, Washington, USA

^hDepartment of Urology, University of Regensburg, Regensburg, Germany

Abstract

Context—The introduction of new lithotripters has increased problems associated with shock wave application. Recent studies concerning mechanisms of stone disintegration, shock wave focusing, coupling, and application have appeared that may address some of these problems.

Objective—To present a consensus with respect to the physics and techniques used by urologists, physicists, and representatives of European lithotripter companies.

[★]Presented in parts at the urolithiasis session at the European Association of Urology Congress, Barcelona, Spain, 17 April 2010.

© 2011 European Association of Urology. Published by Elsevier B.V. All rights reserved

^{*}Corresponding author. Department of Urology, SLK Kliniken Heilbronn, Am Gesundbrunnen 20, D-74074 Heilbronn, Germany. Tel. +49 7131 492401; Fax: +49 7131 492429. jens.rassweiler@slk-kliniken.de (J.J. Rassweiler)..

Author contributions: Jens J. Rassweiler had full access to all the data in the study and takes responsibility for the integrity of the data and the accuracy of the data analysis.

Study concept and design: Rassweiler, Chaussy.

Acquisition of data: Rassweiler, Chaussy, Knoll, Köhrmann, Lingeman, McAteer, Cleveland, Bailey.

Analysis and interpretation of data: Rassweiler, Chaussy, Knoll, Köhrmann, Lingeman, McAteer.

Drafting of the manuscript: Rassweiler.

Critical revision of the manuscript for important intellectual content: Rassweiler, Chaussy, Knoll, Köhrmann, Lingeman, McAteer, Cleveland, Bailey.

Statistical analysis: Rassweiler.

Obtaining funding: None.

Administrative, technical, or material support: None.

Supervision: Rassweiler.

Other (specify): None.

Financial disclosures: I certify that all conflicts of interest, including specific financial interests and relationships and affiliations relevant to the subject matter or materials discussed in the manuscript (eg, employment/affiliation, grants or funding, consultancies, honoraria, stock ownership or options, expert testimony, royalties, or patents filed, received, or pending), are the following: None.

Evidence acquisition—We reviewed recent literature (PubMed, Embase, Medline) that focused on the physics of shock waves, theories of stone disintegration, and studies on optimising shock wave application. In addition, we used relevant information from a consensus meeting of the German Society of Shock Wave Lithotripsy.

Evidence synthesis—Besides established mechanisms describing initial fragmentation (tear and shear forces, spallation, cavitation, quasi-static squeezing), the model of dynamic squeezing offers new insight in stone comminution. Manufacturers have modified sources to either enlarge the focal zone or offer different focal sizes. The efficacy of extracorporeal shock wave lithotripsy (ESWL) can be increased by lowering the pulse rate to 60–80 shock waves/min and by ramping the shock wave energy. With the water cushion, the quality of coupling has become a critical factor that depends on the amount, viscosity, and temperature of the gel. Fluoroscopy time can be reduced by automated localisation or the use of optical and acoustic tracking systems. There is a trend towards larger focal zones and lower shock wave pressures.

Conclusions—New theories for stone disintegration favour the use of shock wave sources with larger focal zones. Use of slower pulse rates, ramping strategies, and adequate coupling of the shock wave head can significantly increase the efficacy and safety of ESWL.

Keywords

Extracorporeal shock wave; lithotripsy; Lithotripter; Shock wave generation; Urolithiasis

1. Introduction

Extracorporeal shock wave lithotripsy (ESWL) is a well-established treatment option for urolithiasis [1–3]. However, the introduction of new lithotripters appears to have increased the potential problems of shock wave application compared with first-generation devices [4,5]. Young urologists favour endourology and are less interested in ESWL, and at several centres, specially trained technicians rather than urologists perform ESWL [6]. Recent studies concerning mechanisms of stone disintegration, shock wave focusing, coupling, and application have appeared that may alleviate some of the problems associated with newer lithotripters. Manufacturers have introduced new devices with significant modifications that, if used appropriately, may also be helpful. In this paper, we present an actual update of all major issues concerning theoretical and practical application of ESWL.

2. Evidence acquisition

This paper is based on discussions held during the 4th Consensus Meeting of the German Shock Wave Lithotripsy Society [7]. In preparation for the meeting, we performed a systematic literature search using the terms extracorporeal shock wave lithotripsy and stone disintegration ($n = 328$), *coupling* ($n = 34$), *shock wave generation* ($n = 179$), and *shock wave induced trauma* ($n = 73$) in Medline, Embase, and PubMed. Inclusion criteria were randomised controlled trials (RCTs), observational series, experimental studies, and reviews providing significant information. Based on this information, we were able to include the expert opinions of participating urologists, physicists, and representatives of European lithotripter companies (Table 1). Finally, the draft of the paper was discussed with American experts in the field of shock wave lithotripsy (James A. McAteer, James E. Lingeman, Robin O. Cleveland, and Michael R. Bailey).

3. Evidence synthesis

3.1. The physics of shock waves

A representative shock wave is shown in Fig. 1. It represents a short-duration ($<10 \mu\text{s}$) acoustic pressure wave consisting of a compressive phase (peak pressure: 30–100 MPa) followed by a tensile phase (negative pressure). From the pressure form, physical parameters can be calculated, such as acoustic energy (E ; Appendix A) and energy flux density (Appendix B). Effective energy (E_{eff}) contributes to fragmentation except for the portion not hitting the calculus. At present, there is a debate on the fragmentation and tissue injury processes, and no clear metric indicates how well a stone will break or how damaged tissue will suffer.

3.2. Mechanism and theories of stone fragmentation

Initial fragmentation, similar to the fracture of any brittle object, represents a process whereby cracks form as a result of stresses generated by applied shock waves [1]. Cracks begin at sites where shock wave–induced stress exceeds a critical value. Further disintegration occurs as a result of growth and coalescence of these cracks under repetitive loading and unloading [8]. Besides established mechanisms describing initial fragmentation like tear and shear forces [1], spallation [9], cavitation [10], and quasi-static squeezing [11], further insight was gained by the studies of Sapozhnikov et al. [12], which introduced the theory of *dynamic squeezing* (Table 2).

3.2.1. Tear and shear forces—If the length of the pulse is smaller than the stone, then because of the geometry of the stone surface and its internal structure, the compressive phase of the shock wave will generate pressure gradients, which can result in shear and tensile stresses in the stone. These stresses can produce tearing and shearing to fragment that stone [1]. In this theory, the shock wave reflection at the stone–water interface, with pressure inversion and splitting off of stone material by the tensile stress of the reflected wave, is emphasised (Fig. 2A).

3.2.2. Spallation—The fluid of the distal stone surface represents an acoustically soft interface, and the leading compressive phase will be reflected as a tensile wave. The amplitude of the tensile stress depends on the difference in acoustic impedance and the geometry of the stone surface. Using high-speed shadowgraphy to image stress waves in translucent model calculi (Fig. 2B), maximum tension occurred within the distal part, resulting in a fracture about a third of the way from the distal end [9,12]. This fracture mechanism is considered similar to freezing water inside a brittle material.

3.2.3. Quasi-static squeezing—If the focal spot is broader than the stone, then pressure waves travel in the fluid along the stone's surface. The leading compressive phase can create circumferential stress, which acts on the stone by quasi-static squeezing, inducing a binary fragmentation with the first cleavage surfaces parallel or perpendicular to the axis of shock wave propagation (Fig. 2C). This process assumes that the shock wave velocity in the surrounding fluid is much lower than the elastic velocities within the stone. The longitudinal shock wave moves through the stone, leaving the thin waves in the fluid encircling and squeezing the stone [11,12]. For squeezing to be effective, the focal width of the lithotripter must be wider than the stone; thus, high fragmentation efficiency will be promoted by large focal diameters up to 20 mm, and it is not necessary for a steep shock front to exist. Data suggest that positive pressure (P_+) could be reduced to 10–30 MPa—sufficient to overcome fracture thresholds (2–10 MPa). This hypothesis has stimulated discussions about the importance of larger focal sizes and lower pressures compared with small focal sizes with high pressures in large-aperture sources [2,13].

3.2.4. Cavitation—In addition to direct shock wave effects, cavitation generated by the negative pressure phase of shock waves occurs in the fluid surrounding stones and within microcracks or cleavage interfaces (Fig. 2D). For initial fragmentation, cavitation is less relevant but becomes important as stone fragments become smaller. Cavitation-induced erosion is especially observed at the anterior surface of stones [10]. Suppression of cavitation using highly viscous media, hyperpressure, or overpressure significantly reduces disintegrative shock wave efficacy [14]. Recognition of the role of cavitation in stone comminution has led to efforts to enhance the action of cavitation bubbles, such as a tandem shock wave generated using a piezoelectric source fitted to an electrohydraulic system, with an additional discharge circuit to produce the second pulse [15]. However, cavitation can be detrimental to fragmentation, as it results in production of gas bubbles lasting for many seconds, therefore attenuating subsequent impulses [16].

3.2.5. Dynamic squeezing—In dynamic squeezing, calculi are fragmented by shear waves created inside the stone driven by squeezing waves from the lateral stone borders (Fig. 2E). The theory is based on a model that accounts for all acoustic phenomena, inside and outside of the calculus, including transmission, reflection, mode conversion, and diffraction [17]. Following predictions from this numerical model, Sapozhnikov et al presented experimental evidence of dynamic squeezing [12], demonstrating that shear waves initiated at the corners of the stone and driven by squeezing waves along the calculus led to the greatest stress, whereas reflection of longitudinal waves at the posterior surface was less important.

3.2.6. Relevance of different theories—Sapozhnikov et al. [12] carried out a set of experiments testing multiple mechanisms on a research lithotripter—spalling, quasi-static squeezing, and cavitation (Table 3). Whereas only one experiment supported spalling and quasi-static squeezing, dynamic squeezing sufficiently described initial fragmentation in all experiments (Appendix C; Fig. 3). Tear and shear forces as well as spallation only remain relevant in small focal sizes. The current consensus is that focal width may play a critical role in stone breakage—at least for initial fragmentation.

3.2.7. Dynamic fatigue—Fragmentation inflicted by shock wave lithotripsy accumulates during the course of treatment, leading to eventual destruction of the stone configuration [8]. Therefore, stone comminution is characterised as a progressive process consisting of initiation (based on dynamic squeezing), propagation (associated with cavitation), and coalescence (because of increasing fragility). Finally, mechanical stresses produce microcracks, resulting in a sudden break-off of the calculus after its molecular structure is destroyed. This theory relates physical stone properties (fracture toughness, acoustic speed, density, void dimensions) to shock wave parameters (peak pressure, pulse width, pulse profile).

3.3. Factors influencing efficacy

According to acoustic properties, shock wave efficacy depends on various factors (Table 4), including how shock waves are generated and the size of the focal zone used.

3.3.1. Generating shock waves—Four generating principles are used in clinical lithotripters. In electrohydraulic lithotripters (EHLs), a spark discharge between two electrodes produces the shock wave. EHLs have a great shot-to-shot variability, as the spark location varies as the electrodes wear down. The significance of this “jitter effect” is under debate [7], with some suggesting that it might be less relevant in large-focus sources [1]. The electroconductive system (EDAP TMS, Vaulx-en-Velin, France) employs electrodes surrounded by a highly conductive solution, resulting in repeatable spark location because of

shorter interelectrode distance and reduced electrode wear [18]. Electrode life time exceeds 40 000 impulses. Electromagnetic and piezoelectric sources provide stable shock wave release lasting for more than a million shocks; however, acoustic output instability may occur [19].

3.3.2. Enlargement and adaptation of the focal zone—In all extracorporeal lithotripters, energy from a large source is focused onto the stone. The size of and peak pressure at the focus depends on the source and the method of focusing (ie, aperture). It is difficult to compare different lithotripters in terms of acoustic output because the range of focal widths and delivered peak pressures is great (Table 1). The classical definition of *focal zone* (the diameter at which the peak pressure is half of P_+ , known as -6 dB) has only minor relevance in describing energy output—namely, the disintegrative efficacy of a source. It is likely that disintegrative efficacy depends on the energy applied to the stone exceeding a specific threshold for stone disintegration, and this requires a more complex calculation (Appendix A).

Some lithotripter manufacturers have found ways to adjust the focal width to suit specific clinical applications. In the MODULITH SLX-F2 urologic workstation (Storz-Medical, Kreuzlingen, Switzerland), two focal sizes are realised by modifying pulse duration using the same electromagnetic source. The larger focal zone (50×9 mm) is recommended for renal stones, and the smaller focus (28×6 mm) is for ureteral stones; however, no improvement in clinical efficacy could be shown [20,21]. The double-layer arrangement of piezoelectric elements in the PiezoLith 3000 lithotripter (Richard Wolf, Knittlingen, Germany) was used to increase shock wave energy after reducing the aperture from 50 cm to 30 cm [22,23]. Modifying synchronisation of both travelling waves additionally allows variation of delay and pulse formation, resulting in three focal zones.

Recent broad-focus, low-pressure lithotripters (LithoSpace [AST, Jena, Germany], lithogold [MTS, Konstanz, Germany], XX-ES [Xi Xin Medical Instruments, Suzhou, PRC]) attracted attention because research showed that focal width affects stone breakage in several ways [24] (Table 1). In vitro [25], the disintegrative efficiency of the XX-ES lithotripter was superior to the HM3 lithotripter (Dornier MedTech Systems, Wessling, Germany; 634 vs 831 shock waves). Because no data of applied energy at different generator voltages (9 kV vs 18 kV) were provided, differences in configuration and acoustic output of both devices must be considered when interpreting results. Siemens and Dornier create larger focal zones by prolonged pulse duration but do not offer different focal sizes [26,27].

3.3.3. Travelling of shock waves—Cavitation bubbles produced by the rarefaction phase of shock waves can decrease the energy of the following impulse through scattering and absorption. Once created, the cavitation bubbles decay in time, so the longer the period until the next shock wave, the fewer bubbles are presented to decrease the energy. Therefore, as the pulse rate frequency (PRF) increases, the number of bubbles in the path increases. It has been shown that increasing the PRF from 1.0 Hz to 1.8 Hz has a drastic effect on shock wave energy [28]. Studies have showed that P_+ is not significantly reduced at fast rates, and only the negative phase is affected [29]. The energy of the negative tail is lost as a result of the growth of cavitation bubbles without affecting P_+ because micro-bubbles persisting between pulses constitute a small volume of field. Also, air bubbles may be created by the mechanical release of oxygen with a much longer lifetime than cavitation bubbles.

3.3.4. Coupling quality—Cost reduction as well as modular and multifunctional lithotripter designs have changed the ideal coupling of the water bath of the HM3 lithotripter to coupling cushions, making coupling quality a key factor in its success (Table 4).

Pishchalnikov et al. [30] demonstrated a linear negative relationship between area occupied by air pockets and shock wave efficiency. Using standardised air bubbles, Bohris revealed that an 8% reduction in coupling area resulted in 43% more impulses in order to retain fragmentation [31]. Jain and Shah [32] examined different coupling media, showing the best fragmentation for bubble-free ultrasound (US) gel compared with low-viscosity silicon oil. Bergsdorf et al. [33] demonstrated that lower viscosity and a greater quantity of gel provided significantly better coupling with respect to fragmentation. Neucks et al. [34] found that applying US gel from a stock container as a large mound was superior to hand or zigzag application from squeezed bottles. Finally, the quality of water cushions can be important, as the membrane can be injured by gel or cleaning substances.

3.3.5. Localisation and monitoring—Stones must be targeted effectively during the delivery of shock waves. This targeting is difficult because respiratory movement can carry the calculus out of the target zone. Immobilisation by high-frequency ventilatory respiration anaesthesia was clinically effective but too invasive. Systems with respiratory belts and shock wave triggering (Lithostar, Siemens, Erlangen, Germany) have been abandoned because of increased treatment time. Cleveland et al. [35] demonstrated the impact of stone movement in an experimental model in which a compression belt may reduce respiratory movement of the kidney [7], and larger focal zones reduce the number of impulses that miss the stone. For lithotripters with smaller focal zones, real-time coaxial US localisation represents the optimal alternative to guarantee adequate coupling and localisation [5,31].

The debate continues as to which imaging system provides the best localisation. Fluoroscopy is the first choice because of the simplicity of isocentric C-arm systems compared with the HM3 lithotripter's in-bath converters (Table 4). Theoretically, inline US is preferable because sound and shock waves travel similarly through the body. Because of acoustic deviation, lateral US may differ from coaxial US (eg, Bohris et al found a 5-mm (range: 3–9) deviation between coaxial/lateral US and fluoroscopy [36]. Duplex US, or acoustic tracking of cavitation, has been used to monitor whether shock waves hit the stone and fragmentation is progressing [37,38].

Automated fluoroscopic localisation (LITHOSKOP [Siemens], Sonolith i-sys [EDAP TMS]) significantly reduces x-ray exposure [18,26]. The Lithotrack system (Storz-Medical)—part of the MODULITH lithotripter—minimises radiation exposure through optical tracking [20], and the correct position of the shock wave source can be controlled using virtual reality without the need for fluoroscopy (Fig. 4A). The LithoSpace lithotripter uses an acoustic tracking system [39] adaptable to US as well as fluoroscopic devices (Fig. 4B).

3.3.6. Impact of pulse rates

3.3.6.1. Experimental studies: Greenstein and Matzkin [40], investigating increasing pulse rates at low and high energy, found that at 2 Hz, 46% more shots were needed for a low-energy setting as compared with 70% for a high-energy setting, suggesting that more cavitation occurred in the shock wave path at high energy levels. Reducing the PRF from 120 to 30 shock waves/min resulted in a pronounced decrease in particle size and an increase in particle surface [41]. In vitro studies show that stone passage rates could be improved from 25% for 2 Hz to 80% for 1 Hz [42]. Slowing the delivery rate from 60 to 30 shock waves/min also provides a dramatic protective effect on the integrity of renal vasculature in a porcine model [43]. These findings support potential strategies of reduced PRF to improve safety and efficacy in ESWL [44].

3.3.6.2. Clinical studies: Low PRF prolongs treatment time significantly and may lead to inconvenience for patients not able to maintain a stable position. The analysis of seven

RCTs ($n = 1235$) suggests a better outcome at 60–80 shock waves/min compared with 120 shock waves/min, most obviously in stones >10 mm in diameter [45–51] (Table 5). To detect significant differences in smaller stones is problematic because the treatment end point is difficult to determine with current imaging techniques.

3.3.7. Application mode—Both in vitro and in vivo studies show advantages in the slow increase of generator voltage (“ramping”) during shock wave lithotripsy [52]. Lower generator voltage results in less pain; thus, patients can better accommodate to treatment under intravenous analgesia. Pretreatment at lower voltages reduces renal trauma by vasoconstriction [53,54]. Lower shock wave pressure is also sufficient to initiate fragmentation. Higher energy is only required to overcome attenuation and scattering effects by fragment collection. At lower energy, less scattering occurs. A recent RCT was able to demonstrate better stone comminution with a ramping strategy [55].

3.3.8. Importance of shock wave energy—As long as the threshold is exceeded, P_+ plays a minor role in stone disintegration, indicating that an overestimation has been placed on P_+ in the past [11,12]. Granz and Köhler [56] had already found that focal shock wave energy represents the relevant parameter for fragmentation. Based on this conclusion, the concept of *energy dose* (E_{dose}) was proposed (Appendix D). Most authors refer to the *power index* (shock wave intensity \times impulses), but this equation does not capture the width of the focal zone. The concept of *effective energy dose* (E_{eff} at intensity level \times impulses) does account for spatial dependence of the acoustic field. In the absence of a better metric, the energy delivered to the stone seems reasonable for enabling comparison of treatment strategies and the effectiveness of lithotripters: The success of ESWL at different intensity levels remains the same when the number of shots delivers an equivalent energy dose. The energy dose for a stone 12 mm in diameter— $E_{\text{dose}}(12 \text{ mm})$ —can be calculated (Appendix C) if sufficient measurements on the lithotripter have been made and the energy dose is compared with outcomes from clinical studies [57–60]. Based on this calculation, the following energy doses are recommended: (1) renal stones: $E_{\text{dose}}(12 \text{ mm}) = 100\text{--}130 \text{ J}$; (2) ureteral stones: $E_{\text{dose}}(12 \text{ mm}) = 150\text{--}200 \text{ J}$.

3.4. Shock wave-induced renal trauma

According to animal experiments as well as kidney perfusion models [61–63], different dose-dependent morphologic findings can be distinguished: Damage of renal parenchyma primarily occurs at vessels and tubular cells. First, venules in the medulla are damaged (grade 1 lesion), followed by rupture of cortical arterioles (grade 2/3 lesion). The mechanical genesis of the initial damage is poorly understood, but hypotheses include tear and shear forces with the microstructure of the tissue [64,65] or cavitation activity in vessels. Zhong et al. [66] have shown that the rupture of artificial vessels was the result of asymmetric expansion of the bubbles along the vessel axis. Chen et al. [67] have shown that bubble collapses in mesentery vessels results in damage to vessel walls.

3.4.1. Cavitation-mediated tissue damage—Basic research reveals a differentiation between cavitation and pressure-induced cell damage. Williams et al. [68] found that 20–50% of cell lysis is produced by shock wave pressure, depending on intensity. Once widespread cavitation has started, it is generally accepted that it dominates the tissue-damage process. For the HM3 lithotripter, it has been reported that it takes about a thousand impulses in a pig model for widespread cavitation to develop [69].

3.4.2. Clinical complications of shock wave lithotripsy—Besides renal injury, ESWL is not completely free from other serious complications, such as gastrointestinal injury in 1.8% of cases, including colonic perforation or duodenal erosions [70]. Matlaga et

al demonstrated the potential for shock waves to damage blood vessels outside the focal zone when the vasculature is seeded with cavitation nuclei [71]. The wide distribution of damage in this study suggests that the acoustic field of a lithotripter delivers negative pressure exceeding cavitation thresholds far off the acoustic axis, underscoring that conditions permissive for cavitation can lead to dramatic sequelae. In contrast, in a large population-based cohort of kidney stone formers, there was no association between ESWL and the subsequent long-term risk of hypertension [72].

3.4.3. Impact of energy flux density—Studies indicate that shear could be the initial insult leading to vessel rupture [65]. In accordance with that idea, the experiments of Bergsdorf demonstrated that energy flux density represents the main parameter of shock wave–induced tissue trauma [63]. Lesion scores only correlated with energy density, not with negative shock wave pressure. Using a clinical dual-head lithotripter (Duet, DirexGroup, Wiesbaden, Germany) with alternating mode and respective reduction of applied energy density (17 kV), Handa et al. [73] observed the same minimal renal lesions compared with the HM3 lithotripter (24 kV). The impact of an electromagnetic self-focussing source with a large focal diameter, long pulse duration, and relatively low peak pressure on renal parenchyma was studied experimentally [25]. The kidneys showed no detectable injury. This result supports a larger focal zone providing similar energy output (correlated to fragmentation) but significantly less energy density (minimising trauma).

We note that for a given shock wave source, energy output and ED increase in parallel as the power level of the lithotripter is increased. In systems allowing creation of different focal zones, ED should be lower in larger focal zones [20–23], although the clinical relevance of such systems remains unclear. In summary, it is practically impossible to increase energy and simultaneously reduce energy flux density.

4. Conclusions

New theories for stone disintegration favour the use of shock wave sources with larger focal zones. The use of slower pulse rates, ramping strategies, and adequate coupling of the shock wave head can significantly increase the efficacy and safety of ESWL (Table 6). All urologists should be aware of new trends and recent results in ESWL research.

Acknowledgments

Funding/Support and role of the sponsor: None.

Appendix A. Acoustic Energy

The acoustic energy (E) of a shock wave pulse for lithotripsy should be determined within an area corresponding to the average size of urinary stones (ie, 12 mm). Effective energy ($E_{\text{eff}}(12 \text{ mm})$) contributing to stone disintegration can be defined as energy delivered to an area 12 mm in diameter in the focal plane. $E_{\text{eff}}(12 \text{ mm})$ is calculated by integrating energy flux density in the focal plane over the area S equivalent to the time integral of the pressure pulse followed by an area integral:

$$E_{\text{eff}}(12\text{mm}) = 2\pi/Z \int_0^{\tau_0} \int_0^{r_0} p^2(r, z_0, t) r dr dt$$

where S is the 12-mm area in the focal plane. Because of the axis symmetry of the shock wave field, it is sufficient to measure the pressure along the x- or y-axis in the focal plane to calculate the energy.

Appendix B. Energy Flux Density

Focal size corresponds to the location where peak pressure P_+ decreases to 50%. Energy flux density includes the temporal pressure of the shock wave—both positive and negative—in the focal plane. In an axis symmetric shock wave field, energy flux density is determined by the integral:

$$ED(r) = 1/Z \int_0^{t_2} P^2(r, z_o, t) dt,$$

where Z is the acoustic impedance of the transmission medium and $z_o = 0$ defines the focal plane. The location in the focal plane is expressed by the radius r from the focal point to the location (x,y) , with the pressure P at this location. Energy flux density can be considered the transmitted shock wave energy at a specific location in the focal plane.

Appendix C. Detailed Description of the Results in the Sapozhnikov et al Study [12]

Only one experiment supported the theory of spallation: the crack occurred a third of the way proximal to the distal end of test stones. Other findings, however, did not support this (Fig. 3; [1]). Partial blockade of the proximal surface (blocking the longitudinal wave) had minimal impact on stone fragmentation, and (2) blocking the lateral wave by a ring significantly lowered the pressure field and disintegrative efficacy. Only one experiment supported the theory of quasi-static squeezing: A baffle ring at the proximal end significantly inhibited stone fragmentation. Static squeezing was not supported in the following experiments (Fig. 3): (1) A conical stone shape significantly inhibited fragmentation, and (2) complete blockade of the stone front significantly inhibited fragmentation.

Appendix D. Energy Dose

The energy dose— $E_{dose}(12\text{ mm})$ —is defined as:

$$E_{dose}(12\text{ mm}) = n E_{eff}(12\text{ mm})$$

where n is the number of applied shocks and $E_{eff}(12\text{ mm})$ is the effective energy—that is, the acoustic energy in the focus per shock wave delivered to an area 12 mm in diameter.

References

- [1]. Chaussy C, Brendel W, Schmiedt E. Extracorporeally induced destruction of kidney stones by shock waves. *Lancet*. 1980; 2:1265–8. [PubMed: 6108446]
- [2]. Fuchs G, Miller K, Rassweiler J, Eisenberger F. Extracorporeal shock-wave lithotripsy: one-year experience with the Dornier lithotripter. *Eur Urol*. 1985; 11:145–9. [PubMed: 4029228]
- [3]. Rassweiler JJ, Renner C, Chaussy C, Thüroff S. Treatment of renal stones by extracorporeal shock wave lithotripsy An update. *Eur Urol*. 2001; 39:187–99. [PubMed: 11223679]
- [4]. Lingeman JE, McAteer JA, Gnessin E, Evan AP. Shock wave lithotripsy: advances in technology and technique. *Nat Rev Urol*. 2009; 6:660–70. [PubMed: 19956196]
- [5]. Rassweiler JJ, Tailly GG, Chaussy C. Progress in lithotripter technology. *EAU Update Series*. 2005; 3(1):17–36.

- [6]. Danuser H, Müller R, Descoeudres B, Dobry E, Studer UE. Extra-corporeal shock wave lithotripsy of lower calyx calculi: how much is treatment outcome influenced by the anatomy of the collecting system? *Eur Urol.* 2007; 52:539–46. [PubMed: 17400366]
- [7]. Rassweiler, JJ.; Bergsdorf, T.; Bohris, C., et al. Consensus: shock wave technology and application—state of the art in 2010. In: Chaussy, C.; Haupt, G.; Jocham, D.; Köhrmann, KU., editors. *Therapeutic energy applications in urology II: standards and recent developments.* Thieme; Stuttgart, Germany: 2010. p. 37-52.
- [8]. Lokhandwalla M, Sturtevant B. Fracture mechanics model of stone comminution in ESWL and implications for tissue damage. *Phys Med Biol.* 2000; 45:1923–40. [PubMed: 10943929]
- [9]. Zhong P, Xi XF, Zhu SL, Cocks FH, Preminger GM. Recent developments in SWL physics research. *J Endourol.* 1999; 13:611–7. [PubMed: 10608511]
- [10]. Crum LA. Cavitation microjets as a contributory mechanism for renal calculi disintegration in ESWL. *J Urol.* 1988; 140:1587–90. [PubMed: 3057239]
- [11]. Eisenmenger W. The mechanisms of stone fragmentation in ESWL. *Ultrasound Med Biol.* 2001; 27:683–93. [PubMed: 11397533]
- [12]. Sapozhnikov OA, Maxwell AD, MacConaghy, Bailey MR. A mechanistic analysis of stone fracture in lithotripsy. *J Acoust Soc.* 2007; 121:1190–202.
- [13]. Rassweiler J, Köhrmann U, Heine G, Back W, Wess O, Alken P. Modulith SL 10/20 - experimental introduction and first clinical experience with a new interdisciplinary lithotripter. *Eur Urol.* 1990; 18:237–41. [PubMed: 2289515]
- [14]. Delius M, Brendel W. A mechanism of gallstone destruction by extracorporeal shock waves. *Naturwissenschaften.* 1988; 75:200–1. [PubMed: 3398924]
- [15]. Zhou Y, Cocks FH, Preminger GM, Zhong P. Innovation in shock wave lithotripsy technology: updates in experimental studies. *J Urol.* 2004; 172:1892–8. [PubMed: 15540748]
- [16]. Pishalnikov YA, Sapozhnikov OA, Williams JC Jr, et al. Cavitation bubble cluster activity in the breakage of kidney stones by lithotripter shock waves. *J Endourol.* 2003; 17:435–46. [PubMed: 14565872]
- [17]. Cleveland RO, Sapozhnikov OA. Modeling elastic wave propagation in kidney stones with application to shock wave lithotripsy. *J Acoust Soc Am.* 2005; 118:2667–76. [PubMed: 16266186]
- [18]. Partheymüller, P. Sonolith i-sys: the new standard in lithotripsy. In: Chaussy, C.; Haupt, G.; Jocham, D.; Köhrmann, KU., editors. *Therapeutic energy applications in urology II: standards and recent developments.* Thieme; Stuttgart, Germany: 2010. p. 65-70.
- [19]. Pishchalnikov YA, McAteer R, VonderHaar J, Pishchalnikova IV, Williams JC, Evan AP. Detection of significant variation in acoustic output of an electromagnetic lithotripter. *J Urol.* 2006; 176:2294–8. [PubMed: 17070315]
- [20]. Wess, O. Storz Medical—shock wave technology for medical applications. In: Chaussy, C.; Haupt, G.; Jocham, D.; Köhrmann, KU., editors. *Therapeutic energy applications in urology II: standards and recent developments.* Thieme; Stuttgart, Germany: 2010. p. 78-81.
- [21]. De Sio M, Autorino R, Quarto G, et al. A new transportable shock-wave lithotripsy machine for managing urinary stones: a single centre experience with a dual-focus lithotripter. *BJU Int.* 2007; 100:1137–41. [PubMed: 17550410]
- [22]. Ginter, S.; Burkhardt, M.; Vallon, P. Richard Wolf: the piezoelectric ESWL—more than 20 years of clinical success worldwide. In: Chaussy, C.; Haupt, G.; Jocham, D.; Köhrmann, KU., editors. *Therapeutic energy applications in urology II: standards and recent developments.* Thieme; Stuttgart, Germany: 2010. p. 87-92.
- [23]. Bölles R, Hoffmann P, Dickmann P, Neisius D. First clinical results of extracorporeal piezoelectric shock wave lithotripsy of kidney and ureteral stones with the Piezolith 3000 with focal zones. *Akt Urol.* 2006; 37:9–12.
- [24]. Eisenmenger W, Du XX, Tang C, et al. The first clinical results of “wide focus and low-pressure” ESWL. *Ultrasound Med Biol.* 2002; 28:769–74. [PubMed: 12113789]
- [25]. Evan AP, McAteer JA, Connors BA, et al. Independent assessment of a wide-focus, low-pressure electromagnetic lithotripter: absence of renal bioeffects in the pig. *BJU Int.* 2007; 101:382–8. [PubMed: 17922871]

- [26]. Lanski, M.; Ulucan, N.; Burnes, L. Lithoskop.: discover the future of urology today. In: Chaussy, C.; Haupt, G.; Jocham, D.; Köhrmann, KU., editors. Therapeutic energy applications in urology II: standards and recent developments. Thieme; Stuttgart, Germany: 2010. p. 71-7.
- [27]. Hofsäß, S.; Rheinwald, M. Dornier MedTech.: update on products for urology. In: Chaussy, C.; Haupt, G.; Jocham, D.; Köhrmann, KU., editors. Therapeutic energy applications in urology II: standards and recent developments. Thieme; Stuttgart, Germany: 2010. p. 57-69.
- [28]. Wiksel H, Kinn AC. Implications of cavitation phenomena for shot intervals in extracorporeal shock wave lithotripsy. *BJU Int.* 1995; 75:720–3.
- [29]. Pishchalnikov YA, Sapozhnikov OA, Bailey MR, Pishchalnikova IV, Williams JC Jr, McAteer JA. Cavitation selectively reduces the negative-pressure phase of lithotripter shock waves. *Acoust Res Lett Online.* 2005; 6:280–6. [PubMed: 19756170]
- [30]. Pishchalnikov YA, Neucks JS, Von der Haar RJ, Pishchalnikova IV, Williams JC Jr, McAteer JA. Air pockets trapped during routine coupling in dry head lithotripsy can significantly decrease the delivery of shock wave energy. *J Urol.* 2006; 176:2706–10. [PubMed: 17085200]
- [31]. Bohris, C. Quality of coupling in ESWL significantly affects the disintegration capacity—how to achieve good coupling with ultra-sound gel. In: Chaussy, C.; Haupt, G.; Jocham, D.; Köhrmann, KU., editors. Therapeutic energy applications in urology II: standards and recent developments. Thieme; Stuttgart, Germany: 2010. p. 61-4.
- [32]. Jain A, Shah TK. Effect of air bubbles in the coupling medium on efficacy of extracorporeal shock wave lithotripsy. *Eur Urol.* 2007; 51:1680–7. [PubMed: 17112655]
- [33]. Bergsdorf T, Chaussy C, Thüroff S. Energy coupling in extracorporeal shock wave lithotripsy—the impact of coupling quality on disintegration efficacy. *J Endourol.* 2008; 22(Suppl):A161.
- [34]. Neucks JS, Pishchalnikov YA, Zancanaro AJ, von der Haar JN, Williams JC Jr, McAteer JA. Improved acoustic coupling for shock wave lithotripsy. *Res Urol.* 2008; 36:61–6.
- [35]. Cleveland RO, Anglade R, Babayan RK. Effect of stone motion on in vitro comminution efficiency of a Storz Modulith SLX. *J Endourol.* 2004; 18:629–33. [PubMed: 15597649]
- [36]. Bohris C, Bayer T, Gumpinger R. Ultrasound monitoring of kidney stone extracorporeal shock wave lithotripsy with an external transducer: does fatty tissue cause image distortions that affect stone comminution? *J Endourol.* 2010; 24:81–8. [PubMed: 19961334]
- [37]. Bohris C, Bayer T, Lechner C. Hit/miss monitoring of ESWL by spectral Doppler ultrasound. *Ultrasound Med Biol.* 2003; 29:705–12. [PubMed: 12754070]
- [38]. Leighton TG, Fedele F, Coleman AJ, et al. A passive acoustic device for real-time monitoring of the efficacy of shockwave lithotripsy treatment. *Ultrasound Med Biol.* 2008; 34:1651–65. [PubMed: 18562085]
- [39]. Hartung, A.; Schwarze, W. LithoSpace by AST GmbH. In: Chaussy, C.; Haupt, G.; Jocham, D.; Köhrmann, KU., editors. Therapeutic energy applications in urology II: standards and recent developments. Thieme; Stuttgart, Germany: 2010. p. 53-6.
- [40]. Greenstein A, Matzkin H. Does the rate of extracorporeal shock wave delivery affect stone fragmentation? *Urology.* 1999; 54:430–2. [PubMed: 10475348]
- [41]. Paterson RF, Lifshitz DA, Lingeman JE, et al. Stone fragmentation during shock wave lithotripsy is improved by slowing the shock wave rate: studies with a new animal model. *J Urol.* 2002; 168:2211–5. [PubMed: 12394761]
- [42]. Pishchalnikov YA, McAteer JA, Williams JC Jr, Pishchalnikova I, vonDerHaar RJ. Why stones break better at slow shock wave rate than at fast rate: in vitro study with a research electrohydraulic lithotripter. *J Endourol.* 2006; 20:537–41. [PubMed: 16903810]
- [43]. Gillitzer R, Neisius A, Wöllner J, et al. Low-frequency extracorporeal shock wave lithotripsy improves renal pelvic stone disintegration in a pig model. *BJU Int.* 2009; 103:1284–8. [PubMed: 19159409]
- [44]. McAteer JA, Evan AP, Williams JC Jr, Lingeman JE. Treatment protocols to reduce renal injury during shockwave lithotripsy. *Curr Opin Urol.* 2009; 19:192–5. [PubMed: 19195131]
- [45]. Davenport K, Minervini A, Keoghane S, Parkin J, Keeley FX. Does rate matter? The results of a randomized controlled trial of 60 versus 120 shocks per minute for shock wave lithotripsy of renal calculi. *J Urol.* 2006; 176:2055–8. [PubMed: 17070254]

- [46]. Madbouly K, El-Tiraifi AM, Seida M, El-Faqiu SR, Atasi R, Talic RF. Slow versus fast shock wave lithotripsy rate for urolithiasis: a prospective randomized study. *J Urol.* 2005; 173:127–30. [PubMed: 15592053]
- [47]. Yilmaz E, Batislam E, Basar M, Tuglu D, Mert C, Basar H. Optimal frequency in extracorporeal shock wave lithotripsy: prospective randomized study. *Urology.* 2005; 66:1160–4. [PubMed: 16360432]
- [48]. Pace KT, Ghiculete D, Harju M, Honey RJ, University of Toronto Lithotripsy Associates. Shock wave lithotripsy at 60 or 120 shocks per minute: a randomized, double-blind trial. *J Urol.* 2005; 174:595–9. [PubMed: 16006908]
- [49]. Chacko J, Moore M, Sankey N, Chandhoke PS. Does slower treatment rate impact the efficacy of extracorporeal shock wave lithotripsy for solitary kidney or ureteral stones? *J Urol.* 2006; 175:1370–3. discussion 1373–4. [PubMed: 16515999]
- [50]. Kato Y, Yamaguchi S, Hori J, Okuyama M, Kakizaki H. Improvement of stone comminution by slow delivery rate of shock waves in extracorporeal lithotripsy. *Int J Urol.* 2006; 13:1461–5. [PubMed: 17118017]
- [51]. Koo V, Beattie I, Voung M. Improved cost-effectiveness and efficiency with a slower shock wave delivery rate. *BJU Int.* 2010; 105:692–6. [PubMed: 19888982]
- [52]. Weizer AZ, Zhong P, Preminger GM. New concepts in shock wave lithotripsy. *Urol Clin North Am.* 2007; 34:375–82. [PubMed: 17678987]
- [53]. Seemann O, Rassweiler J, Chvapil M, Alken P, Drach GW. The effect of single shock waves on the vascular system of artificially perfused rabbit kidneys. *J Stone Disease.* 1993; 5:172–8. [PubMed: 10146235]
- [54]. Willis LR, Evan AP, Connors BA, Handa RK, Blomgren PM, Lingeman JE. Prevention of lithotripsy-induced renal injury by pretreating kidneys with low-energy shock waves. *J Am Soc Nephrol.* 2006; 17:663–7. [PubMed: 16452495]
- [55]. Lambert EH, Walsh R, Moreno MW, Gupta M. Effect of escalating versus fixed voltage treatment on stone comminution and renal injury during extracorporeal shock wave lithotripsy: a prospective randomized trial. *J Urol.* 2010; 183:580–4. [PubMed: 20018316]
- [56]. Granz B, Köhler G. What makes a shock wave efficient in lithotripsy? *J Stone Dis.* 1992; 4:123–8. [PubMed: 10149177]
- [57]. Sorensen C, Chandhoke P, Moore M, Wolf C, Sarram A. Comparison of intravenous sedation versus general anesthesia on the efficacy of the Doli 50 lithotripter. *J Urol.* 2002; 168:35–7. [PubMed: 12050487]
- [58]. Tailly GG. In situ SWL of ureteral stones: comparison between an electrohydraulic and an electromagnetic shock wave source. *J Endourol.* 2002; 16:209–14. [PubMed: 12042101]
- [59]. Lalak N, Moussa SA, Smith G, Tolley DA. The Dornier Compact Delta lithotripter: the first 500 renal calculi. *J Endourol.* 2002; 16:3–7. [PubMed: 11890447]
- [60]. Lalak N, Moussa SA, Smith G, Tolley DA. The Dornier Compact Delta lithotripter: the first 150 ureteral calculi. *J Endourol.* 2002; 16:645–8. [PubMed: 12490016]
- [61]. Rassweiler J, Köhrmann KU, Back W, et al. Experimental basis of shockwave-induced renal trauma in the model of the canine kidney. *World J Urol.* 1993; 11:43–53. [PubMed: 8490667]
- [62]. Koehrmann KU, Back W, Bensemann J, et al. The isolated perfused kidney of the pig: new model to evaluate shockwave induced lesions. *J Endourol.* 1994; 8:105–10. [PubMed: 8061665]
- [63]. Bergsdorf T, Thüroff S, Chaussy C. The isolated perfused kidney: an in vitro test system for evaluation of renal tissue by high-energy shockwave sources. *J Endourol.* 2005; 19:883–8. [PubMed: 16190851]
- [64]. Evan AP, McAteer JA, Connors BA, Blomgren PM, Lingeman JE. Renal injury in SWL is significantly reduced by slowing the rate of shock wave delivery. *BJU Int.* 2007; 100:624–7. [PubMed: 17550415]
- [65]. Freund JB, Colonius T, Evan AP. A cumulative shear mechanism for tissue damage initiation in shock-wave lithotripsy. *Ultrasound Med Biol.* 2007; 33:1495–503. [PubMed: 17507147]
- [66]. Zhong P, Zhou Y, Zhu S. Dynamics of bubble oscillation in constrained media and mechanisms of vessel rupture. *Ultrasound Med Biol.* 2002; 28:661–71. [PubMed: 12079703]

- [67]. Chen H, Kreider W, Brayman AA, Bailey R, Matula TJ. Blood vessel deformations on microsecond time scales by ultrasonic cavitation. *Phys Rev Lett*. 2011; 106:34301.
- [68]. Williams JC Jr, Jason JF, Woodward MA, Stonehill MA, Evan AP, McAteer JA. Cell damage by lithotripter shock waves at high pressure to preclude cavitation. *Ultrasound Med Biol*. 1999; 25:473–9. [PubMed: 10374989]
- [69]. Bailey MR, Pishchalnikov YA, Sapozhnikov OA, et al. Cavitation detection during shock wave lithotripsy. *Ultrasound Med Biol*. 2005; 31:1245–9. [PubMed: 16176791]
- [70]. Maker V, Iayke J. Gastrointestinal injury secondary to extracorporeal shock wave lithotripsy: a review of the literature since its inception. *Am Coll Surg*. 2004; 198:128–35.
- [71]. Matlaga BR, McAteer JA, Connors BA, et al. Potential for cavitation-mediated tissue damage in shockwave lithotripsy. *J Endourol*. 2008; 22:121–6. [PubMed: 18315482]
- [72]. Krambeck AE, Rule AD, Li X, Bergstralh EJ, Gettman M, Lieske C. Shock wave lithotripsy is not predictive of hypertension among community stone formers at long-term followup. *J Urol*. 2011; 185:164–9. [PubMed: 21074794]
- [73]. Handa RK, McAteer JA, Evan AP, Connors BA, Pishchalnikov YA, Gao S. Assessment of renal injury with a clinical dual head lithotripter delivering 240 shock waves per minute. *J Urol*. 2009; 181:884–9. [PubMed: 19095269]

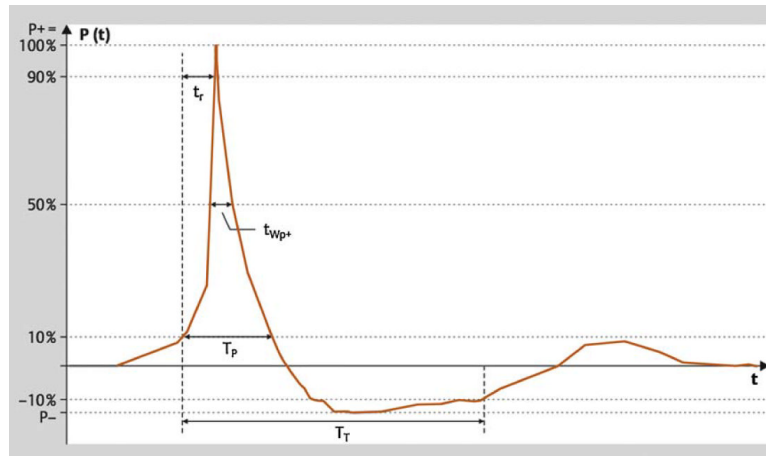


Fig. 1.

Typical shock wave pulse form in the focal zone. There is a rapid pressure increase at t_0 to a peak pressure value P_+ , with the rise time t_r followed by a decrease to zero crossing the zero line at t_1 and a negative phase P_- until t_2 . The time interval t_0 to t_1 is denominated a positive pulse duration t_{p+} . P_+ varies according to the intensity settings of the shock wave generator. The pulse width t_w is defined as the time during which peak pressure is $>50\%$ of P_+ . The pressure profile $P(x,y,z,t)$ describes shock waves in one specific location of the pressure field. The focal width is defined according to the -6 -dB contour in the x and y direction.

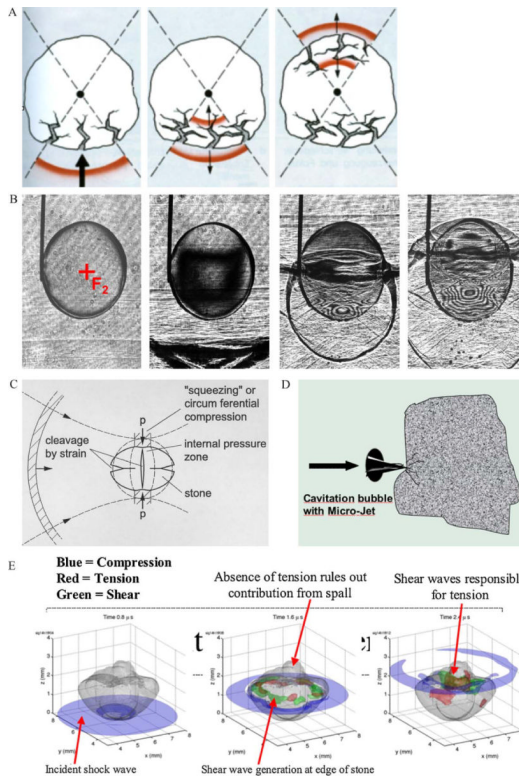


Fig. 2. Different theories for initial stone fragmentation. (A) Tear and shear forces: Shock waves are transmitted and reflected at the low impedance stone-water interfaces, with pressure inversion splitting off stone material by tensile stress. (B) Spalling: The distal stone surface as an acoustically soft interface generates a reflected tensile wave of the initially compressive longitudinal shock wave pulse propagating through the calculus, with maximum tension within the distal third of the stone (high-speed shadowgraphy by Zhong). (C) Quasi-static squeezing: Stone breakage by tensile stress of the circumferential shock wave resulting from a lower shock wave velocity in the surrounding fluid than within the stone (modified from Eisenmenger). (D) Cavitation: Negative pressure waves of high-speed shocks cause cavitation in liquids surrounding stones and within microcracks or cleavage interfaces by inducing microjets. (E) Dynamic squeezing: Shear waves initiated at the corners of the stone and driven by squeezing waves along the calculus lead to the greatest stress and tension (three-dimensional computer simulation according to a numerical model by Cleveland). Note the different pressure distributions and travelling time of waves inside and along the stone surface. *Blue = compressive phase; green = maximum shear stress (55 MPa); red = maximum tensile stress (80 MPa).

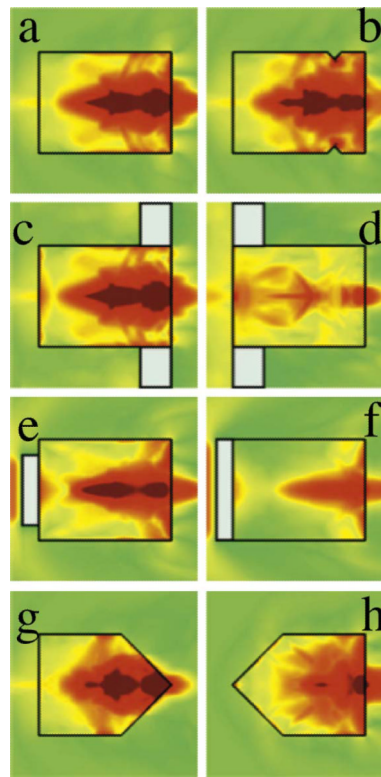


Fig. 3. Stress fields in the different stone experiments using a research lithotripter patterned after the Dornier HM3 system (Sapozhnikov et al. [12]). The maximal stress field (a) is little changed by blocking the longitudinal wave entering the stone (e) or altering the distal end of the stone (b,c,g). However, blocking the circumferential squeezing wave alone (d) or preventing the creation of shear waves at the corners (f, h) significantly reduces the intensity of stress.

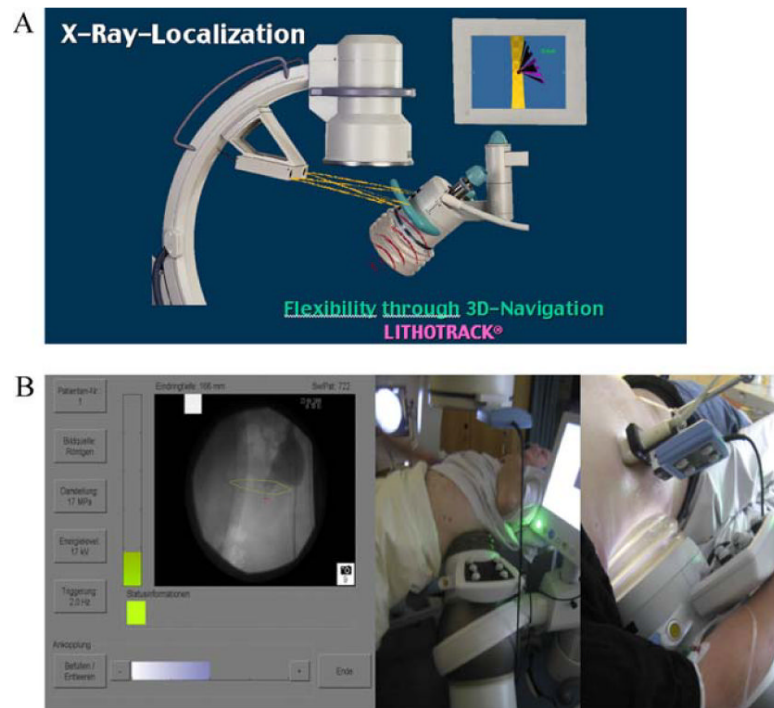


Fig. 4. Navigation for stone localisation. (A) Optical tracking: A camera system checks the position of the shock wave source arranged with an isocentric fluoroscopic C-arm (Lithotrack). (B) Acoustic tracking: Sound waves of six piezoelectric sources attached to the shock wave source are tracked by six receivers attached to the localisation system, which was calibrated previously. The focal zone is displayed on the screen (SuperVision, AST).

Table 1

Comparison of technical details of new lithotripters

| Lithotripter | Shock wave generation | Focal size (-6 dB) Lateral (mm) | Focal depth (mm) | Maximum pressure (MPa) | Localisation system | Features |
|-------------------------------|---|--|------------------|------------------------|--|---|
| Siemens LITHOSKOP | Electromagnetic (coil; pulse) | 12 | 160 | N/A* | Isocentric fluoroscope C-arm Inline ultrasound | Shock wave source on parallel isocentric C-arm Multifunctional working station |
| Domier Doli S | Electromagnetic (coil; EMSE, 220) | 6 | 150 | 90 | Isocentric fluoroscope C-arm Inline ultrasound Lateral ultrasound | Three simultaneous localisation options (tri-mode) |
| Storz-Medical MODULITH SLX-F2 | Electromagnetic (cylinder) | F1: 6 F2: 9 | 180 | 150 90 | Inline fluoroscopy Inline ultrasound | Two focal sizes Multifunctional working station |
| Xi Xin XX-ES | Electromagnetic (self-focusing) | 18 | 180 | 30 | Lateral ultrasound | Low-pressure ESWL Large focus |
| EDAP TMS Sonolith i-sys | Electroconductive (Diatron IV) | 14 | 170 (155-210) | N/A | Isocentric fluoroscope C-arm Isocentric ultrasound | No jitter effect Automatic pressure regulator |
| MTS Lithogold 380 | Electrohydraulic (SmartTrode) | 16 | 165 | 40 | Adaptable to a C-arm | Low-pressure ESWL Large focus |
| AST LithoSpace | Electrohydraulic | 17 | 140 | 38 | Adaptable to a C-arm and ultrasound | Navigation with acoustic tracking (Super-Vision) |
| Richard Wolf PiezoLith 3000 | Piezoelectric (two self-focussing layers) | F1: 2 F2: 4 F3: 8 | 165 | 126 119 48 | Isocentric fluoroscope C-arm Inline ultrasound | Three focal sizes Dual simultaneous localisation |

N/A = not available; ESME = estimated mean square error; ESWL = extracorporeal shock wave lithotripsy.

* E12 mm; 117 mJ.

Table 2

Summary of existing theories for stone fragmentation

| Hypothesis | Mechanism | Prerequisites | Type of action | Comments |
|-----------------------------|---|---|---|--|
| Tear and shear forces [1] | Pressure gradients resulting from impedance changes at the stone front and distal surface with pressure inversion | Shock wave smaller in space extension than the stone | Hammer-like action resulting in a crater-like fragmentation at both ends of the stone | Only relevant for small focus zones |
| Spallation [9] | Reflected tensile wave at distal surface of the stone with maximum tension at the distal part of the stone | Shock wave smaller in space extension than the stone | Breaking the stone from the inside like freezing water in brittle material | Only relevant for small focus zones No explanation for stone breakage at the front side |
| Quasi-static squeezing [11] | Pressure gradient between circumferential and longitudinal waves results in squeezing of the stone | Shock wave is broader than the stone Shock wave velocity is lower in the water than in the stone | Nutcracker-like action requiring large focal diameters | Only relevant for large focal zones |
| Cavitation [10] | Negative pressure waves induce a collapsing cavitation bubble at the stone surface | Low viscosity of surrounding medium | Microexplosive erosion at the proximal and distal ends of the stone | More important during stone comminution Useful for improving the efficiency of shock waves (ie, EHL) |
| Dynamic squeezing [12] | Shear waves initiated at the corner of the stone are reinforced by squeezing waves along the calculus | Parallel travelling of longitudinal waves Shock wave velocity is lower in the water than in the stone | Nutcracker-like action in combination with spalling | Best theory to explain results of the numerical model |

EHL = electrohydraulic lithotripter.

Table 3

Models and results of the experimental evaluation of stone fragmentation by shock waves (according to Sapozhnikov et al.[12])

| Mechanism | Model | Hypothesis | Stone model/numerical calculation |
|------------------|--|--|---|
| Spallation | Stone length: 8–18 mm | Stone fractures at the same distance from the distal end | Stone fractures at a third of the way from the distal end dependent on length |
| | Block of proximal surface by corprene disk | Stone fracture is significantly inhibited | Little difference (50 vs 45 shock waves) Pressure field similar at the last third |
| Squeezing | Baffle ringing the proximal end | Stone fracture is significantly inhibited | Significant inhibition (300 vs 45 shock waves) but reduced stress field still at the last third |
| | Conical shape of the stone front | Stone fracture is not inhibited | Significant inhibition (200 vs 45 shock waves) Pressure field reduced because of diffraction |
| | Block of proximal end (complete) | Stone fracture is not inhibited | Significant inhibition (212 vs 45 shock waves) Pressure field reduced because of absorption |

Table 4

Factors influencing the success of extracorporeal shock wave lithotripsy

| Factor for success | Options | Specific modifications | Advantages | Comments/problems |
|-------------------------------------|---|---|--|--|
| Shock wave generation and focussing | Electrohydraulic with ellipsoid reflector | Spark electrode | Large focus | Variability of pulses One electrode per session |
| | | Twin heads | Lower energy density | Coupling from two sites is difficult |
| | | Electroconductive | No variability of pulses 40 000 shock waves | - |
| | Electromagnetic | Coil membrane with acoustic lens | Extension of focal zone by prolonged pulse duration | Advantage of larger focal zone not clinically proven |
| | | Cylinder with paraboloid reflector | Dual focus by different pulse duration (ie, for renal and ureter stones) | Advantage of dual focus not clinically proven |
| Coupling of shock waves | Piezoelectric | Spherical element | Very large focal zone | Not available in Europe |
| | | Spherical alignment with two layers | Three focal sizes | Advantage of triple focus not clinically proven |
| | Water bath | Complete (Dornier HM3) | Ideal coupling | No multifunctional use |
| | | Partial (EDAP TMS Sonolith 2000, Richard Wolf PiezoLith 2200) | | No longer manufactured |
| Water cushion | Gel pad (abandoned) | | Multifunctional use | 20% attenuation of shock wave energy |
| | | Coupling gel | | Warm ultrasound gel from container High amounts on cushion Shave skin of patient Check quality of coupling by inline ultrasound |
| | | | | |
| Stone localisation | Fluoroscopic C-arm | Automated positioning | Reduction of x-ray exposure | Fluoroscopy first choice worldwide |
| | Inline fluoroscopy | Optical tracking | Reduction of x-ray exposure | Camera checks position of shock wave source |
| | | Acoustic tracking | Adaptation to external C-arm | Five piezoelectric elements track the position of the shock wave source |
| | Inline ultrasound | - | Real-time shock wave application Control of coupling quality | Difficult in obese patients and midureteral stones |
| Lateral ultrasound | Tri-mode localisation system (isocentric) | - | | 5 mm tolerance (range: 3–9 mm) to inline ultrasound |

Table 5

Randomised controlled trials (evidence level Ib/A) comparing different pulse rates for extracorporeal shock wave lithotripsy

| Study | No. (slow/fast) | Lithotriptor | Pulse rates, No./min | No. of impulses, slow vs fast | Overall SFR at 3 mo, % | SFR, 3 mo, % | | Comments |
|-----------------------|-----------------|---|----------------------|-------------------------------|------------------------|-----------------|-----------------|---|
| | | | | | | <10 mm | 10–20 mm | |
| Pace et al. [48] | 220 (111/109) | LithoTron (Healthtronics, Atlanta, GA, USA) | 60 vs 120 | 2423 vs 2906 | 60 vs 45 | 60 vs 49 (n.s.) | 60 vs 28 | Double-blind RCT Only SSA >100 mm ² significant |
| Yilmaz et al. [47] | 170 (56/57/57) | StoneLitho3pter (PCK, Ankara, Turkey) | 60 vs 90 vs 120 | 3037 vs 2989 vs 3019 | N/A | N/A | N/A | Success rate (<3-mm fragments) 73% vs 88% vs 89% |
| Madbouly et al. [46] | 156 (76/80) | Lithostar Multifline (Siemens) | 60 vs 120 | 5755 vs 7414 | 85 overall | N/A | N/A | Success rate (<2-mm fragments) 99% vs 90% Stone size most important for success |
| Chacko et al. [49] | 349 (171/178) | DoLi-50 (Dornier) | 70–80 vs 120 | 2428 vs 2785 | N/A | 65 vs 57 (n.s.) | 67 vs 46 | Difficult to determine treatment endpoint in small stones |
| Davenport et al. [46] | 104 (50/54) | DoLi S (Dornier) | 60 vs 120 | 3000 vs 3000 | 49 vs 47 (n.s.) | 59 vs 61 (n.s.) | N/A | No difference related to a stone area of 60 mm ² |
| Kato et al. [50] | 134 (66/68) | MODULITH SLX (Storz-Medical) | 60 vs 120 | 6348 vs 6348 | 77 vs 76 (n.s.) | 83 vs 75 (n.s.) | 65 vs 79 (n.s.) | Desintegration rate 65% vs 47% |
| Koo et al. [51] | 102 (51/51) | DoLi S (Dornier) | 70 vs 100 | 3045 vs 4414 | 67 vs 26 | N/A | N/A | Cost reduction resulting from slow rate |
| Total | 1235 | - | - | - | - | - | - | - |

SFR = stone-free rate; RCT = randomised controlled trial; n.s. = not significant; SSA = stone surface area (length × width); N/A = not applicable.

Table 6
Therapeutic recommendations for extracorporeal shock wave lithotripsy (energy level for the Siemens LITHOSKOP)

| Stone size, mm | Location | No. of shock waves | Energy level* | Frequency, shock waves/min | Comments |
|----------------|----------|--|---|---|---|
| 5–10 | Kidney | 3000–3500 | Ramping: 100 shock waves with Level 0.1–1 Afterwards, maximal level: Lower calyx: 3.0 Upper and middle calyx: 3.5 Pelvis: 4.0 | 60 | Check BP (maximum systolic BP: 140 mm Hg) Retreatment after 2–3 d |
| | Ureter | 3500–4500 | No dose escalation (ramping) Maximal Level: Upper ureter: 4.0 Middle ureter: 6.0 Distal ureter: 8.0 | Upper and middle ureter: 90 Distal ureter: 120 | Retreatment after 2 d Minimal movement of distal ureteral stone |
| 10–20 | Kidney | Single stone: 3500 Multiple stones: 4000 (ie, 2 × 2000) | Ramping: 100 shock waves with level 0.1–1 Afterwards, maximal level: Lower calyx: 3.0 Upper and middle calyx: 3.5 Pelvis: 4.0 | 60 | Check BP (max. systolic BP: 140 mm Hg) Start with the smallest stone Retreatment after 2–3 d |
| | Ureter | 4500 | No dose escalation (ramping) Maximal level: Upper ureter: 4.0 Middle ureter: 6.0 Distal ureter: 7.0 | Upper and middle ureter: 90 Distal ureter: 120 | In case of no stent, start at the upper rim Minimal movement of distal ureteral stones |

BP = blood pressure.

* 8–117 mJ/impulse (measured by light-spot hydrophone).